International Journal of Advanced Research in Physical Science (IJARPS)
Volume 5, Issue 11, 2018, PP 1-14
ISSN No. (Online) 2349-7882
www.arcjournals.org

Some Problems of Modeling the Volume Processes of Relaxed Optics

Petro P. Trokhimchuck

Department of Theoretical and Mathematical Physics, Lesya Ukrayinka East European National University, 13 Voly Avenue, Lutsk, Ukraine.

Corresponding Author:** ***Petro P. Trokhimchuck, *Department of Theoretical and Mathematical Physics, Lesya Ukrayinka East European National University, 13 Voly Avenue, Lutsk, Ukraine.*

Abstract: *Problems of modeling the volume processes of Relaxed Optics are discussed. It was shown that these processes may be having nonequilibrium and irreversible nature. Bond between radiated and non-radiated relaxation or processes of Nonlinear and Relaxed Optics is observed. Physical-chemical and electrodynamics' aspects of these phenomena are analyzed. Modified Rayleygh models and Bohrs theory of Cherenkov radiation are used for the observation of represented experimental data. Comparative analysis the methods of modeling shock waves processes and cascade model of excitation in regime of saturation the excitation are used for modeling the laser-induced breakdown of irradiated matter. Corresponding experimental data are analyzed too*

Keywords: *Nonlinear Optics, Relaxed Optics, volume processes, saturation of excitation, cascade processes, irreversible phenomena, Cherenkov radiation, shock waves.*

1. INTRODUCTION

Problem of modelling volume processes of Relaxed Optics (RO) is connected with problem of increasing lifetime of basic elements of optoelectronic systems, including semiconductors, optical fibers and other [1, 2].

In whole this problem [1 – 5] is very complex problem. It connected with various nature of relaxation of first-order optical excitation. It may be simple two-three-stage, cascade, cyclic or more complex relaxation. Processes of radiative and nonradiative relaxation generally interconnected, they cause each other. First (radiative) processes are processes of Nonlinear Optics (NLO). Second (nonradiative) processes are processes of Relaxed Optics. Therefore we must use various old methods and create new methods of modeling of these processes and phenomena.

Therefore relaxed optical processes may be cause of nonlinear optical processes and conversely nonlinear optical processes may be cause of relaxed optical processes. Roughly speaking relaxed optical processes are the trace of interaction oh the light and matter in matter. Establishing the order of these processes is one of the most difficult problems of modeling mixed processes of relaxed optics. We must determine time, geometry and chain of proper processes.

Examples of mixing processes and phenomena of RO are pulse Ruby and Neodimium laser implantation of indium antimonide [1, 2]; cascade processes of the creation the laser-induced structures, including processes of laser sublimation and ablation [1, 2].

Basic NLO phenomena are connected with processes of intrinsic light scattering (absorption) on stable or metastable centers. So, the concentrations these centers in solid are equaled ~ 10^{15}–10^{17} cm^{-3}. Therefore we can use adiabatic approximation and basic formalisms of NLO are perturbation theory and nonlinear differential and integral equations. According by H. Haken [6] NLO phenomena may be represented as nonequilibrium second-order phase transitions. This idea was developed and expanded on Relaxed Optics in [5].

Relaxed Optics (RO) is the chapter of modern physics of irreversible interaction light and matter [1, 2]. Necessity of creation RO is caused of technological applications of laser radiation (laser annealing, laser implantation and other [2]). Phenomenological energy-time and electromagnetic classifications of processes and phenomena of interaction light and matter are basis of RO. According to energy-time classification we have three types of processes and phenomena: kinetic (mainly quantum first-order

processes); dynamic (mainly wave second-order processes) and mixing kinetic-dynamic or dynamic-kinetic processes. Properly to this concept we can have three types phase transformations: kinetic, dynamic and more complex cascade kinetic-dynamic or dynamic-kinetic processes. Really it is photochemical, plasmic, thermal and mixing phenomena [2].

Thermal and plasmic processes are the field processes and for the light scattering in matter it are second order processes. Therefore the time of formation of these processes is more as time of first-order quantum processes (photochemical or photocrystall chemical). Hierarchy of this times is next: time of optical excitation – $10^{-18}-10^{-15}$ s, time of local (quantum) electromagnetic relaxation – $10^{-15}-10^{-12}$ s, time of generation of plasmic oscillations – $10^{-13}-10^{-10}$ s, "thermal" times of heating and cooling – $10^{-9}-10^{-5}$ s [2]. First two processes are primary and quantum processes, last two processes are secondary.

Primary processes are caused of mechanisms of light scattering and local microscopic relaxation, secondary – macroscopic relaxation mechanisms. Therefore we must include these results for the explanation of real picture of interaction light and matter.

Observation the volume laser-induced phase transformations processes (experimental data) was begin by Hersher [7] and first system researches were represented in B. Sharma PhD thesis [8].

Therefore methods for modeling of the laser-induced surface and volume phase transformations are various. This fact is caused of different conditions of radiation: self-absorption for surface and intrinsic absorption for volume. In first case we may have processes of one or two photon processes and for second case – multiphotonic processes. The problems of creation the volume laser-induced phase transformations are another as creation the surface laser-induced phase transformations. This is represented on example of experimental data of volume laser-induced phase transformations in 4H-SiC [9, 10]. Influences of processes the multiphoton absorption and impact ionization are observed.

The proper models (Lugovoy-Prokhorov theory of moving foci [11 – 15] and modified Rayleygh models [5, 16 – 20]) may be used for the explanation of receiving experimental data. Possible application the cascade model for the representation these results is analysed too. The supercontinuum spectra of laser-induced filaments may be explain with help Bohrs theory [21 – 24] of Cherenkov radiation.

2. EXPERIMENTAL DATA

First experimental data of irreversible interaction the laser radiation and semiconductors were received by M. Birnbaum in 1965 [25]. He observed the surface interferograms after pulse Ruby-laser irradiation of germanium, silicon, indium antimonite a.o. [25]. These results are beginning of researches of surface laser-induced phase transformations. The first system volume laser-induced phase transformations systematically are represented in [8] by B. S. Sharma. He observed laser-induced damages in glasses after pulse Ruby laser irradiation.

Now we represent of some experimental data of RO, which will model. We select laser-induced surface volume phase transformations, which are connected with various mechanisms of light absorption. It allows observing basic peculiarities of proper physical processes and methods of its modeling.

In [9, 10] for minituarization of receiving structures of crystals 4H-SiC were irradiated by pulses of femtosecond laser (duration of pulses 130 *fs*, wavelength 800 *nm*, frequency of pulses 1 *kHz*, density of energy 200-300 *nJ*/pulse) with help microscope (Fig. 1).

Conditions of irradiation are represented in Fig. 1 ((a), (b)) [9]. Femtosecond laser pulses were irradiated along the lines inside 4H-SiC single crystals at a depth of 30 μm by moving the sample at a scan speed of 10 $\mu m/s$. The laser beam was irradiated at a right angle to the (0001) surface of the crystal. The irradiated lines were almost parallel to the $\left[1\bar{1}00\right]$ direction. A schematic illustration of the laser-irradiated pattern is shown in Fig. 1 (a). The distance between neighboring lines was 20 μm.

Bright-field TEM (transmission electron microscopy) image of the cross section of a line written with a pulse energy of 300 *nJ*/pulse is shown on Figure 1 ((c) – (e)) [9, 10].

In contrast to the formation of surface periodical structures three-dimensional periodic structures were obtained in this case. Sectional area of these structures was ~ 22 μm, the depth of ~ 50 μm. As seen

from Fig. 1(c) we have five stages disordered regions, which are located at a distance from 2 to 4 μm apart vertically [9]. Branches themselves in this case have a thickness from 150 to 300 *nm*. In this case there are lines in the irradiated nanocavity spherical diameter of from 10 *nm* to 20 *nm*. In this case irradiated structures have crystallographic symmetry of the initial structure.

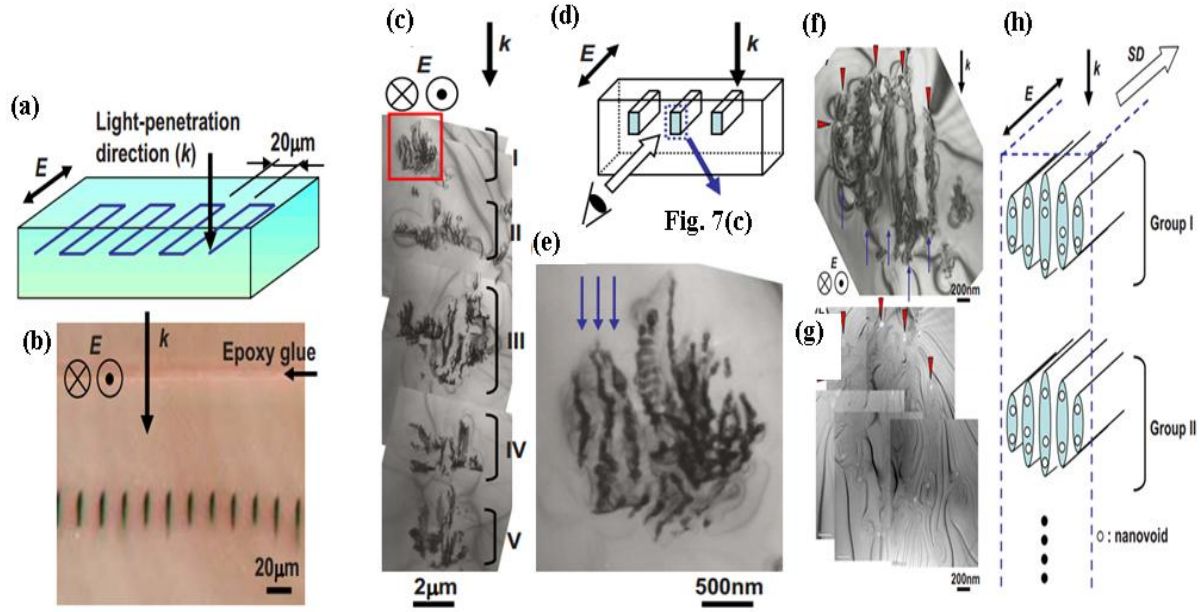

Fig1. *(a) Schematic illustration of the laser irradiated pattern. The light propagation direction (k) and electric field (E) are shown. (b) Optical micrograph of the mechanically thinned sample to show cross sections of laser-irradiated lines (200 nJ/pulse). (c) Bright-field TEM image of the cross section of a line written with pulse energy of 300 nJ/pulse. (d) Schematic illustration of a geometric relationship between the irradiated line and the cross-sectional micrograph. (e) Magnified image of a rectangular area in (c). Laser-modified layers with a spacing of 150 nm are indicated by arrows. (f) Bright-field TEM image of a portion of the cross section of a line written with a pulse energy of 200 nJ/pulse. (g) Zero-loss image of a same area as in (f) with nanovoids appearing as bright areas. Correspondence with (f) is found by noting the arrowheads in both micrographs. (h) Schematic illustrations of the microstructure of a laser modified line. Light-propagation direction (k), electric field (E), and scan direction (SD) are shown. Only two groups (groups I and II) of the laser-modified microstructure are drawn [9, 10].*

More detail information about processes, which are generated in first two stages, represents in Fig. 1 ((f) – (h)) [10].

The research of extensive measurements of damage thresholds for fused silica and calcium fluoride at 1053 and 526 nm for pulse durations τ ranging from 270 fs to 1 ns [26, 27] is represented in Fig. 2.

The explanation of experimental results of Fig. 2, which is represented in [26], is next. In the long-pulse regime (τ > 20 ps), the data fit well by a $\tau^{1/2}$ dependence, characteristic of the transfer of electron kinetic energy to the lattice and diffusion during the laser pulse. The damage is thermal in nature and characterized by the melting and boiling of the surface (Fig. 3 (a)). The damage occurs over the entire area irradiated. For long pulses, heating of the lattice and subsequent thermal damage can occur without significant collisional ionization. For pulses shorter than 20 ps, the damage fluence no longer follows $\tau^{1/2}$ dependence and exhibits a morthology dramatically different from that observed with long pulses. The damage appears as a shallow fractured and pitted crater characteristic of thin layers of material removed by ablation (Fig. 3(b)). Furthermore, short-pulse damage is confined to a small region at the peak of Gaussian irradiance distribution, where the intensity is sufficient to produce multiphoton ionization. With insufficient time for lattice coupling, there no is collateral damage. As a result, it can be many order of magnitude smaller with short (τ < 10 ps) pulses than with long pulses. For the case of fused silica shown in Fig. 3, the damages area produced by the 500 fs pulse was two orders of magnitude smaller than that produced by the 900 ps pulse.

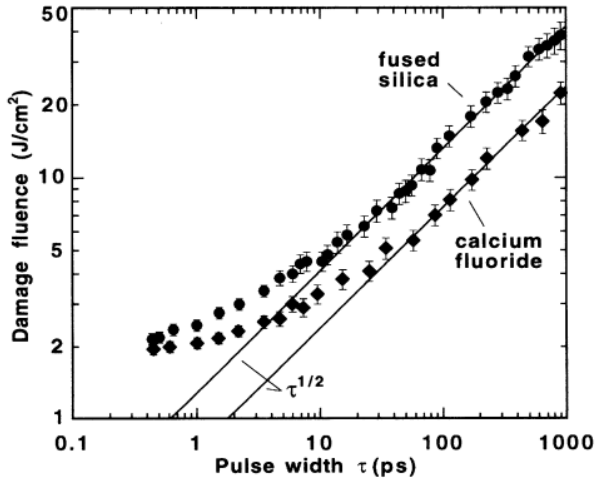

Fig2. *Observed values of damage threshold at 1053 nm for fused silica (●) and calcium fluoride (◆). Solid lines are $\tau^{1/2}$ fits to long pulse results. Estimated uncertainty in the absolute fluence is ±15 % [26, 27].*

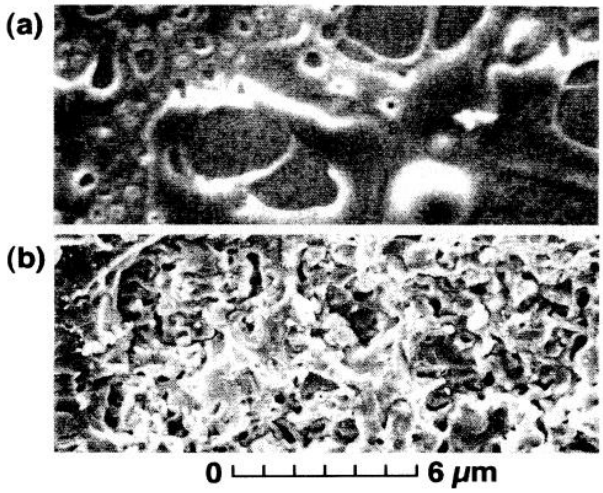

Fig3. *Scanning electron micrograth of front-surface damage of fused silica produced by 1053 nm pulses of duration (a) 900 ps, showing melting, and (b) 500 fs, showing ablation and fracture [26].*

3. MODELING AND DISCUSSIONS

The methods of modeling the phase transformations in Relaxed Optics must be based on the concept of saturation of excitation, which is basic for laser physics and theory of phase transitions [2 – 5]. H. Haken used this analogy for the modeling Nonlinear Optical phenomena as nonequilibrium phase transitions [6]. But classic Nonlinear Optical processes is processes of nonequilibrium impurities light scattering in solid with impurity concentration 10^{15} – 10^{16} cm^{-3}. In this case we have radiated relaxation (effects of Linear and Nonlinear Optics) [27, 28]. For case of self-absorption we can have radiated and unradiated relaxation. The last is cause of Relaxed Optical Processes [2, 5]. Therefore we accented attention on this moment for the explanation experimental data of Fig. 1 – Fig. 3.

Explanation of the experimental data, which are shown in Figure 1 is based on nanoplasmic model [9, 10]. The emergence nanovoids explained on the basis of the explosive mechanism. However, the same result can be explained by the formation of vacancy clusters, especially those sizes of nanovoids same are equivalence to sizes of nanoclusters [5]. Nanovoids, as a rule, are formed between the most modified regions, i.e. in these areas there are sinks of vacancies [29], which form the nanovoids or vacancies clasters.

But we can select basic peculiarities of experimental data of Fig. 1: 1) cascade character of laser-induced phase transformations (Fig. 1 (c)); 2) conic form of each term of cascade (Fig. 1 (c) and Fig 1 (e)); 3) short length of “channels” of optical breakdown (Fig. 1 (e)). Therefore our modeling must include these three facts.

However, it turned out that self-focusing, including filamentation, is accompanied by conical radiation with a spectrum width of up to 8000 cm^{-1} [13]. By its nature, this radiation resembles the Cherenkov radiation [21 – 24], especially if viewed from a microscopic point of view. Therefore, we must to clarify the nature of the conical radiation of self-focusing and its connection with the Cherenkov radiation [21 – 24]. It may be answer on second peculiarity (conic form of each term of cascade (Fig. 1 (c) and Fig 1 (e)).

The appearance of the conical part of the radiation can be explained on the basis of the microscopic nature of the Cherenkov radiation [21 – 22]. The first to draw attention to this were Niels and Aage Bohr [7], and their theory was developed by I.M. Frank and his student A.P. Kobzev [23, 24]. From this point of view, Cherenkov radiation is the inelastic radiation loss of the energy of the incident particle in the matter [21 – 24], or in other words, the response of the matter to its polarization by the incident particle.

Fig. 4 shows the scheme that underlies in the N. Bohr theory [21, 22].

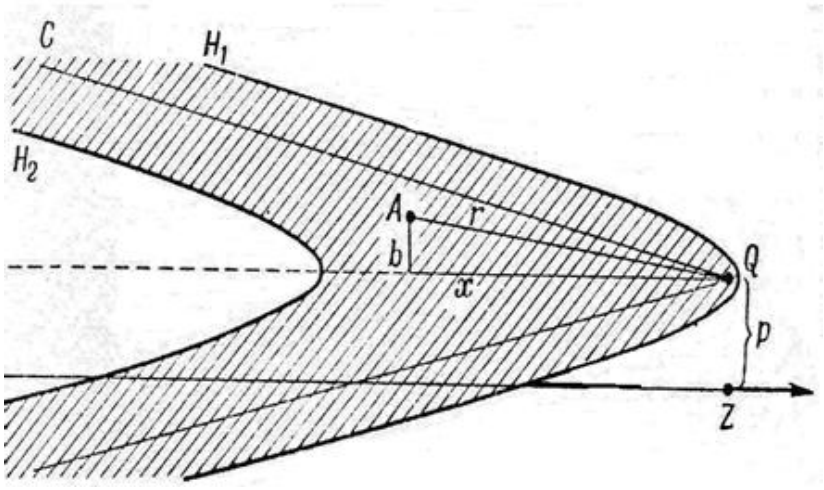

Fig4. *To the explanation of the deceleration the particle in a medium [21, 22].*

We will explain on the basis of Fig. 4. Consider an electron that is at a point Q and collides with a particle Z that flies at a distance p. At the same time, the electron is under the influence of the electrons surrounding it, and those electrons that at the moment of time $t' = t - r/c$ were themselves accelerated give the greatest part of the influence.

The electron at the point A at time t 'was in such a phase of collision, which is ahead during time τ the phase of collision of an electron that is at point Q. This lead time is equal to [21, 22]

$$\tau = \frac{r}{c} - \frac{x}{\vartheta}. \tag{3}$$

Introduce $r^2 = x^2 + b^2$ (Fig.5), we receive from (3) the next correlation

$$\frac{b^2}{\tau^2 c^2 \left(\gamma^2 - 1\right)} - \frac{\left(x + \vartheta\tau\gamma^2\right)^2}{\vartheta\tau\gamma^2\left(\gamma^2 - 1\right)} = 1, \tag{4}$$

The next conclusion is true: points with a constant τ are placed on a hyperboloid. The electrons that "started" or "ended" collisions are placed approximately on hyperboloids H_1 and H_2, that corresponds to the times $\tau = -\frac{p}{2\gamma\vartheta}$ and $\tau = +\frac{p}{2\gamma\vartheta}$. Thus the main part of the force with which a matter acts on an electron is between the hyperboloids H_1 and H_2. For the $\gamma >> 1$ main part of this region is placed behind the electron at a distance equal or greater than $p\gamma$.

The radiation itself occurs in the angle between the perpendiculars to the surface of the hyperboloid, which corresponds to both the angle of the Cherenkov radiation and its broadband. We present a

formal theory of this phenomenon according to [21, 22]. In this case, the transverse part of the field (between the perpendiculars to the hyperboloid) is characterized by a vector potential, which expands into a Fourier series

$$\vec{A}_{tr} = \sum_{\lambda} q_\lambda \vec{A}_\lambda + q_\lambda^* \vec{A}_\lambda^*, \quad \vec{A}_\lambda = \sqrt{4\pi c^2}\,\Omega^{-1/2}\vec{e}_\lambda e^{i(\vec{k}_\lambda \vec{r})}, \tag{5}$$

where values with an asterisk denote complex conjugate values. Here it is assumed that the field is localized in the volume Ω; and the unit vector $\vec{e}_\lambda$ gives the direction of polarization. Amplitudes q_λ in formula (5) are not fully determined; they must satisfy even some of the conditions imposed on their dependence on time.

In the approximation of the constant dielectric constant and neglecting the magnetic properties of the matter, we obtain the following equation

$$\Delta\vec{A} - \frac{\varepsilon}{c^2}\frac{\partial^2 \vec{A}}{\partial t^2} = -\frac{4\pi \vec{j}}{c}, \tag{6}$$

where $\vec{j}$ is the current density, which corresponds to a moving particle; ε – dielectric constant of the matter. After multiplying equation (6) by $\vec{A}_\lambda^*$ and integrating over the volume Ω, we get

$$\left(\ddot{q}_\lambda + \ddot{q}_{-\lambda}^*\right) + \omega_\lambda^2\left(q_\lambda + q_{-\lambda}^*\right) = \frac{z_1 e}{\varepsilon c}\left(\vec{\vartheta}\cdot\vec{A}_\lambda^*(x)\right), \tag{7}$$

where x characterizes the position of the particle, which is considered to be a point charge. Frequencies are given by the formula

$$\omega_\lambda = \frac{k_\lambda c}{\sqrt{\varepsilon}}. \tag{8}$$

Next, we assume that the amplitude q_λ dependence on time is harmonic $\exp(-i\omega_\lambda t)$. As a result of this substitution, equation (7) takes the form

$$\ddot{q}_\lambda + \omega_\lambda^2 q_\lambda = \frac{z_1 e}{2\varepsilon c}\left(1 + \frac{i}{\omega_\lambda}\frac{d}{dt}\right)\left(\vec{\vartheta}\cdot\vec{A}_\lambda^*(x)\right). \tag{9}$$

If the particle moves at a constant speed, then for $x = \vartheta t$ the right side of equation (9) it will harmonically depend on time with frequency $\left(\vec{k}_\lambda \vec{\vartheta}\right)$. Equation (9) is reduced to the following equation

$$\ddot{q}_\lambda + \omega_\lambda^2 q_\lambda = \frac{z_1 e}{2\varepsilon c\left\{\left(\vec{k}_\lambda \vec{\vartheta}\right)\right\}}\left(1 + \frac{\left(\vec{k}_\lambda \vec{\vartheta}\right)}{\omega_\lambda}\right)\left(\vec{\vartheta}\cdot\vec{A}_\lambda^*\left(\vec{\vartheta}t\right)\right). \tag{10}$$

Thus, in this particular case, the dispersion of the medium can be taken into account. Only according to equation (10) it is necessary to substitute the value for the dielectric constant, which corresponds to the partial frequency.

As follows from equation (8), in the vacuum the value $\omega_\lambda > \left(\vec{k}_\lambda \cdot \vec{\vartheta}\right)$, is as $\vartheta < c$. In this case, the solution of equation (10) will be forced oscillations with constant amplitude. However, in metter with $\vartheta > c$ for some wave numbers, we can get $\omega_\lambda = \left(\vec{k}_\lambda \cdot \vec{\vartheta}\right)$, what corresponds to the resonance between the external force and the oscillator. In this case, the oscillator will continuously absorb energy, which corresponds to the actual Cherenkov radiation. The resonance condition, which is described by formula (8), corresponds to the Cherenkov radiation angle [21, 22].

Using the Dirac functions, the general solution of equation (10) can be written as follows

$$q_\lambda = \frac{z_1 e}{2c\omega_\lambda}\frac{1}{\varepsilon\left\{\left(\vec{k}_\lambda \vec{\vartheta}\right)\right\}}\left(\frac{1}{\omega_\lambda - \left(\vec{k}_\lambda \vec{\vartheta}\right)} + i\pi\delta\left(\omega_\lambda - \vec{k}_\lambda \vec{\vartheta}\right)\right)\left(\vec{\vartheta}\cdot\vec{A}_\lambda^*\left(\vec{\vartheta}t\right)\right). \tag{11}$$

Using equation (11), we determine the force $\vec{F}_{tr}$ that acts on the particle.

$$\vec{F}_{tr} = -\frac{z_1 e}{c}\dot{\vec{A}}_{tr}\left(\vec{\vartheta}t\right) = -\frac{z_1 e}{c}\sum_{\lambda}\dot{q}_{\lambda}\vec{A}_{\lambda}\left(\vec{\vartheta}t\right) + \dot{q}^{*}_{\lambda}\vec{A}^{*}_{\lambda}\left(\vec{\vartheta}t\right), \tag{12}$$

That according (5) and (11) give

$$\vec{F}_{tr} = -4\pi^2 z_1^2 e^2 \Omega^{-1}\sum_{\lambda}\vec{e}_{\lambda}\left(\vec{e}_{\lambda}\cdot\vec{\vartheta}\right)\frac{\left(\vec{k}_{\lambda}\cdot\vec{\vartheta}\right)}{\omega_{\lambda}^2\left\{\left(\vec{k}_{\lambda}\cdot\vec{\vartheta}\right)\right\}}\delta\left(\omega_{\lambda} - \left(\vec{k}_{\lambda}\cdot\vec{\vartheta}\right)\right). \tag{13}$$

Summing in two directions of polarization, introducing $\left(\vec{k}_{\lambda}\cdot\vec{\vartheta}\right) = k_{\lambda}\vartheta y$ and moving to an infinitely large volume we get [21, 22]

$$F_{tr} = z_1^2 e^2 \int_0^{\infty} k^2 dk \int_{-1}^{+1} \frac{k\vartheta^2 y}{\omega\varepsilon\left(k\vartheta y\right)}\left(1-y^2\right)\delta\left(\omega - k\vartheta y\right)dy, \tag{14}$$

where F_{tr} is the force component in the direction of the particle velocity.

In calculating the integral (14), we turn to the new variables, ω and $z = \frac{\vartheta}{c}y\sqrt{\varepsilon\left(k\vartheta y\right)}$. Since $\vartheta dxdy = d\omega dz$, we get

$$F_{tr} = \frac{z_1^2 e^2}{c^2}\int_0^{\infty}\omega d\omega\int z\left(1-\frac{c^2}{\vartheta^2\varepsilon\left(\omega z\right)}\right)\delta\left(1-z\right)dz, \tag{15}$$

where the last integral is extended to the values of z, for which $-1 < \frac{cz}{\vartheta\sqrt{\varepsilon\left(\omega z\right)}} < 1$. This integral is nonzero only for z = 1, i.e. when the condition is met $\vartheta\sqrt{\varepsilon\left(\omega\right)} > c$.

Thus, we finally get the value of the force acting on the particle.

$$F_{tr} = \frac{z_1^2 e^2}{c^2}\int_{\vartheta\sqrt{\varepsilon}>c}\left(1-\frac{c^2}{\varepsilon\vartheta^2}\right)\omega d\omega, \tag{16}$$

It coincides with the expression obtained by Frank and Tamm for the Vavilov-Cherenkov radiation and its spectral distribution [21, 22].

The creation of five groups of nanovoids (Fig. 1(c)) is caused of "moving" focus in irradiated matter, which is connecting with processes of blooming at the irradiation time [11 – 15]. These results may be represented as trace of Lugovoy-Prokhorov theory of moving focuses in irradiated matter [11 – 15].

The using of moving focus for explanation results of Fig. 1 isn't necessary because laser radiation is focused with help microscope. But second part of this theory may be used for the explanation basic peculiarities of experimental data Fig. 1. The creation of frozen filaments of Fig. 1 (e) – (g) may be explained on the basis nonlinear diffraction theory and cascade model of laser-induced phase transformations. This hypothesis is certified the almost linear characters of formation the frozen filaments. Process creation of new phases is begun on the rings of maximum the diffractive pattern. But creation of new phases (optical break-down frozen nanofilaments) is indentical to creation the surface laser-induced micro and nanostructures. The stratification of diffractive ring on these filaments are caused of the creation new phases, which are "creator" these frozen nanofilaments. Threfore the stratification of laser irradiation on various zones in the Lugovoy-Prokhorov model of moving focuses may be explained with help theory of creation the diffractive pattern. But in nonlinear case the maximums of this pattern may be have more large density of energy.

But roughly speaking the direction of nanofilaments is corresponded to direction of self-trapping. These irreversible nanofilaments may be represented as nanotrace of self-trapping in irradiated matter too.

According to the generalizing model of moving foci [11] filament is represented the continuum set of nonlinear foci in temporal layers of pulse, beginning from pulse with maximal power. In this case temporal layers of pulses aren't independent and redistribution of its structural intensityis determined of the processers the plasma generation in previous layers, in which intensity attained the photoionization threshold. In the time of filamentation the Kerr nonlinearity is the basic for leading edge of a pulse and plasma instability, which is cause the defocusing, is the basic for falling edge of pulse.

The optical break-down of matter may be explained on the basis of cascade model: multiphoton processes of light absorption in the regime of saturation the excitation of proper scattering centers [30 – 32].

The cone character the one knot of Fig. 1(c) or Fig. 1 (e) may be represented as frozen pattern of Cherenkov radiation with optical pumping []. The angle 2θ at the pick of Fig. 5 or Fig 1(e) is corresponded to the Cherenkov angle oe angle of Mach cone [33]. According to these data next conclusion may be made: the creation of cascade of destructions is connected of the shock ionization and this effect is analogous to microscopic mechanism of Cherenkov radiation [33]. But this angle is greater as Cherenkov angle

$$\sin\theta_{ch} = \frac{1}{n}, \tag{17}$$

where n – refractive index. For 4H-SiC n = 2,77 [34] $\theta_{ch} = 21^{\circ}$. Greater value of angle θ maybe explain of two ways: 1) on the basis of nonlinear defocusing of initial radiation and 2) increasing of Cherenkov angle for nonlinear regime of irradiation ("optical pumping" of hyperboloid of Fig. 4) [33].

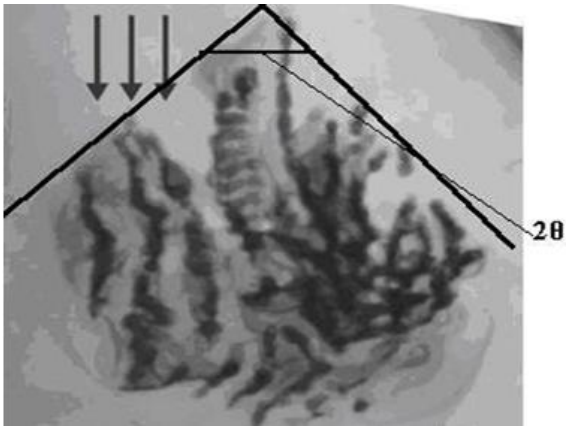

Fig5. *Magnified image of a rectangular area in Fig. 1(e). Angle 2θ is equaled to the Cherenkov angle [33].*

The appearance of the nonlinear-optical self-focusing effect is due to the G.A. Askaryan, V.I. Talanov and Ch.Towns with colleagues theories [11 – 15, 28]. If in the G.A. Askaryan and V.I. Talanov researches considered the question of the propagation of a powerful laser beam with a Gaussian cross section in a medium, and the basis of a more Ch. Townes and his colleagues complete theory of the phenomenon were M. Harper's experimental results on the production of filamentary structures in glass after irradiation with a ruby laser pulse [28]. In the Ch. Towns studies, the conditions for the appearance of self-channeling were obtained, which ultimately made it possible to explain the appearance of filamentary damage [33]. Although the first experimental confirmation of self-focusing are N.F. Pilipetsky and A.R. Rustamov results [33]. The theory of the effect is very simple: when a beam propagates with a Gauss cross section, the refractive index changes over its cross section, which leads to self-focusing, and in the particular case to self-channeling [28, 33].

Similar processes occur during irradiation of the medium with ultrashort pulses. This suggests the conclusion that the broadband part of self-focusing corresponds to the Cherenkov radiation. What is common here is a change in the polarization properties of the matter, both when a high-energy particle passes through a substance and during self-focusing. The hyperboloid of Fig. 4 is similar to the Gaussian distribution of radiation in the TEM_{00} laser mode and distribution of focusing laser radiation too. However, if during the passage of high-energy particles with the same energy, we have many

hyperboloids, then with the passage of a laser pulse, which causes the appearance of self-focusing, such a "hyperboloid" is one. Due to the fact that laser radiation excites unequal polarization over its cross section, the above model of N. Bohr and A. Bohr [21, 22] can be successfully used to explain conical radiation during self-focusing. In this case, it is necessary to take into account the change in the dielectric constant during photoionization of the medium by laser radiation and the fact that the transverse part is exactly the same radiation as for high-energy particles. In other words, the cone radiation of self-focusing can be considered as Cherenkov radiation with "optical pumping".

The reason for filamentation [13] (formation of filaments 50–80 μm in diameter and with length of several tens of meters in propagation of collimated femtosecond laser pulses in air) is the formation of small-scale self-focusing, which can be caused by the formation of induced diffraction gratings and moving foci [13]. This phenomenon is also associated with the breakdown of air and by its nature is obviously similar to the formation of lightning, only in our case the ionization (breakdown) of the air layer is performed on one side due to multiple narrowly directed photoionization taking into account the processes of reradiation.

In a solid, the filaments are smaller in size, due to the higher density of the matter and are observed in the volume destruction of dielectrics (glass and quartz) [5]. From the physicochemical point of view, these processes can also be described by the methods of Relaxed Optics [5] (multiphoton ionization in the excitation saturation regime).

Roughly speaking the explanation of experimental data of Fig. 1 © is next: the creation cascade of volume destruction is "trace" of moving foci. Each stage of this cascade (Fig. 5) is result of creation the shock optical breakdown in "Mach cone". The mechanism of creation new phase of irradiated matter is similar to surface case. In surface case we have generation of surface nano or microcolumns which are perpendicularly oriented to irradiated surface. For volume case (Fig. 1 and Fig. 5) the nanofilaments are oriented parallel to axe of "Mach cone". Wave character of these nanofilaments is corresponded to crystal nature of irradiated matter.

The answer on first peculiarity of the experimental data of Fig. 1 (c) may be next. The estimation of sizes the cascade of volume destructions maybe explains in next way. The sizes (diameters) of proper stages d_{nir} of cascade are proportionally to corresponding diffraction diameters (diameter of proper diffraction circle) d_{ndif}

$$d_{nir} = kd_{ndif}\ , \tag{18}$$

where k is the proportionality constant.

The diffraction diameters d_{ndif} may be determined with help condition of diffraction-pattern lobes (modified Rayleygh ratio)

$$d_{ndif} = n\lambda. \tag{19}$$

The estimations of diffraction diameters d_{ndif} for λ = 800 *nm* are represented in Table 1.

Table1.

n	1	2	3	4	5
d_{ndif} , *nm*	800	1600	2400	3200	4000

The data of Table 1 for n=1, 2, 3 allow to explain of sizes the first three stages of cascade the volume destruction (Fig. 1 (c)). For this case coefficient k ~ 2. But for stages 4 and 5 of Fig. 1 (c) our estimations $k_4 \sim 1{,}2$ and $k_5 = 1$. Various values of coefficients k_i are explained of various conditions of optical breakdown and creation proper phase transformations.

The distance between diffraction spots and proper "moving" foci may be determined with help next formula

$$l_{nf} = \frac{d_{ndif}}{2\tan\varphi/2}. \tag{20}$$

These distances for φ_1 = 20° and φ_2 = 30° are represented in Table 2.

Table2.

n	1	2	3	4	5
l_{nf} , nm for $\varphi_1 = 20^o$	2269	4538	6807	9076	11345
l_{nf} , nm for $\varphi_2 = 30^o$	1493	2985	4478	5970	7463

Qualitative explanation of development of cascade the destructions may be next. The focus of each diffraction zone (spot) is the founder proper shock optical breakdown. But foci with more high number may placed in the "zone" of influence of previous foci. Therefore only first stage of Fig. 1 (c) is represented pure shock mechanism (Mach cone). Mach cones are characterized the second and third stages of Fig. 1 (c). But its maximums are displaced from center. It may be result if interaction second and third shock waves with previous shock waves: first – for second wave and first and second for third wave. The chock mechanism of destruction certifies a linear direction of optical breakdown. This direction is parallel to direction of shock wave and radiated spectrum is continuum as for Cherenkov radiation and as for observed laser-induced filaments in water and air [13]. Thus basic creator of optical breakdown traces is secondary Cherenkov radiation and shock waves. This radiation is absorbed more effectively as laser radiation and therefore the creation of optical breakdown traces is more effectively as for beginning laser radiation. Cherenkov radiation is laid in self-absorption range of 4H-SiC, but 800 nm radiation – in intrinsic range. For the testing of this hypothesis we must measure the spectrum of secondary radiation. In this case we can use physical-chemical cascade model of excitation the proper chemical bonds of irradiated matter in the regime of saturation the excitation.

We can rough estimate basic peculiarities of energy distribution in Mach cone.

Now we estimate the basic energy characteristics of experimental data, where are represented in Fig. 1 ©. Let each stage of cascade has ~200 nanotubes with sizes – d_{nt} =20 nm in diameter and with length l_{nt} = 500 nm. General number of these nanotubes is $N_{1\text{snt}}$ ~ 1000. Its summary volume has value

$$V_{1snt} = N_{1snt} \frac{\pi d_{nt}^{\ 2}}{4} l_{nt} = 0,63 \mu m^3. \tag{21}$$

The average atom density of 4H-SiC may be determined with help next formula

$$N_a = \frac{\rho N_A}{A}, \tag{22}$$

where ρ – density of semiconductor, N_A – Avogadro number, A – a weight of one gram-atom. For 4H-SiC $N_{aSiC} = 2,4 \cdot 10^{22}\ cm^{-3}$.

Number of atoms in summary volumes of nanotubes is equalled

$$N_{asnt} = N_{aSiC} V_{1snt} = 1,51 \cdot 10^{10}. \tag{23}$$

Energy, which is necessary for the optical breakdown our nanotubes may be determined in next way. Zeitz threshold energy for 4H-SiC is equaled E_{Zth} ~ 25 eV [29, 35, 36]. Let this value is corresponded to energy of optical breakdown. Therefore summary energy E_{1ob} is equaled

$$E_{1ob} = N_{asnt} \cdot E_{Zth} = 30,2\ nJ. \tag{24}$$

This value is equaled of 10% from pulse energy. In this case we have more high efficiency of transformation initial radiation to Cherenkov radiation. It is result of more intensive excitation comparatively with classical methods of receiving the Cherenkov radiation. In this case we have pure photochemical processes. The experimental data for intrinsic absorption (Fig. 2) show that for short pulse regime of irradiation (femtosecond regime) basic processes of destruction the fused silica and calcium fluoride are photochemical (multiphoton absorption in the regime of saturation the excitation). But basic peculiarity of experimental data Fig.1 is transformation the initial laser radiation (wavelength 800 nm) to continuum Cherenkov radiation. From length of optical breakdown in 4Y-SiC we can determine average absorption index of Cherenkov radiation. It is ~ 10^4 cm^{-1}. This value is

corresponded to violet-blue range of absorption spectrum of 4H-SiC (band gap of 4H-SiC is equaled 3, 26 eV) [34]. It is corresponded to ultraviolet and range of absorption spectrum of 4H-SiC [34].

The questions about supercontinuum radiation in the process of femtosecond laser filamentation are discussed in [13]. In air supercontinuum spectra laid from ultraviolet to infrared ranges of spectra. In whole nonlinear optics of filaments is included the super expansion of frequency-angle spectrum of initial pulse, generation of more higher harmonics and terahertz irradiation, pulse compression, optical anisotropy of filament and other nonlinear phenomena [13].

In solid this spectrum must be displaced to ultraviolet range? Therefore our traces of filaments have more little length as in water or air [13].

Modified Raylegh and cascade models are addition to Lugovoy-Prokhorov theory of moving foci.

Nanovoids may be represented as results of the laser-induced laser-induce breakdown and creation of cavitation bubbles [16, 17, 37 – 40] too. The light pressure may be determined with help of next formula [8]

$$p_0 = \frac{E_{ir}}{\tau_i c S}, \tag{25}$$

where E – energy of irradiation, τ_i – pulse duration, S – area of irradiation zone, c – speed of light. For circle symmetry

$$S = \pi r^2, \tag{26}$$

where r – radius of laser spot.

For the estimations of maximal radius of nanovoids we must use modified Rayleygh formula [5, 16, 17]

$$R_{\max} \approx \frac{T_c}{0,915}\sqrt{\frac{p_0}{\rho_0}}, \tag{27}$$

where T_c – the time of creation the nanovoid (bubble), ρ_0 – the density of irradiated matter.

Time T_c may be determined as

$$T_c \approx \frac{d_c}{\vartheta_s}, \tag{28}$$

where d_c – characterized size of nanovoid (cavitation bubble), ϑ_s – speed of sound. For the spherical symmetry $d_c = 2R$, where R is radius of nanovoid.

The speed of sound may be determined as [5, 41]

$$\vartheta_s = \sqrt{\frac{E}{\rho_o}}, \tag{29}$$

where E – Young module.

The finished formula for determination $R_{\max}$ has next form [5]

$$R_{\max} \approx \frac{2R}{0,915r}\sqrt{\frac{E_{ir}}{\pi\tau_i c E}}. \tag{30}$$

If we substitute r = 250 *nm*, R = 10 *nm*, E=600 *GPa* [35, 36], E_{ir}=130 *nJ*, τ_i = 130 *ps*, c=3·10^8 *m/s*, than have $R_{\max}$=11 *nm*.

The speed of shock waves for femtosecond regime of irradiation is less as speed of sound. But we have two speeds of sound in elastic body: longitudinal ϑ_{ls} and transversal ϑ_{ts} [41]. Its values are determined with next formulas

$$\vartheta_{ls} = \sqrt{\frac{E(1-\nu)}{\rho_o(1+\nu)(1-2\nu)}}, \text{ and } \vartheta_{ts} = \sqrt{\frac{E}{2\rho_o(1+\nu)}}, \tag{31}$$

where ν – Poisson's ratio . The ratio between of these two speeds is equaled

$$\alpha = \frac{\vartheta_{ts}}{\vartheta_{ls}} = \sqrt{\frac{(1-2\nu)}{2(1-\nu)}}. \tag{32}$$

But this ratio must be true for shock waves too. Therefore for silicon carbide for ν = 0,45 [35, 6] α = 0,33. Roughly speaking last ratio is determined the step of ellipsoidal forms of our nanovoids (Fig. 1h).

For more précised modeling we can use average speed of sound

$$\vartheta_{ms} = \frac{1}{2}(\vartheta_{ls} + \vartheta_{ts}) = \frac{1}{2}\left[\frac{\sqrt{2E(1-\nu)} + \sqrt{E(1-2\nu)}}{\sqrt{2\rho_0(1+\nu)(1-2\nu)}}\right]. \tag{33}$$

In general case this value must be multiplied on Mach number M.

After this remarks finished formula for determination of $R_{\max}$ may be represented in the next form

$$R'_{\max} = \frac{4R\sqrt{2E_{ir}(1+\nu)(1-2\nu)}}{0,915r\sqrt{\pi c\tau_i M}\left[\sqrt{2E(1-\nu)} + \sqrt{E(1-2\nu)}\right]} = 2\frac{\sqrt{2(1+\nu)(1-2\nu)}}{\sqrt{M}\left[\sqrt{2(1-\nu)} + \sqrt{(1-2\nu)}\right]}R_{\max}. \tag{34}$$

For our case and for we have M=1 $R'_{\max} = 0,75R_{\max}$. But Much number has more value as one for millisecond and nanosecond regimes of irradiation and less value of one for femtosecond regime. Therefore we have tolerable coincidence of modeling and experimental data [16, 17].

We can estimate $R_{\max}$ for longitudinal ϑ_{ls} and transversal ϑ_{ts} speeds of light too. These formulas have next forms

$$R_{\max l} = \sqrt{\frac{(1+\nu)(1-2\nu)}{(1-\nu)}}R_{\max} \approx 0,51R_{\max},\ R_{\max t} = \sqrt{2(1+\nu)}R_{\max} \approx 1,7R_{\max}. \tag{35}$$

Parameter α from (32) may be determined as

$$\alpha = \frac{R_{\max l}}{R_{\max t}} = 0,33 \tag{32a}$$

too.

But formulas (35) allow estimating maximal longitudinal and transversal $R_{\max}$. This values are 6 nm and 19 nm properly.

In this case we represented 4H-SiC as isotropic plastic body. For real picture we must represent hexagonal structure. But for the qualitative explanation of experimental data of Fig. 1 this modified Rayleygh model allow explaining and estimating the sizes and forms of receiving nanovoids.

Thus we give answer on three peculiarities of experimental data of Fig. 1 with help of experimental data of Fig. 2 and Fig. 3 and represented models are explained the basic volume processes and phenomena of Relaxed Optics.

4. CONCLUSIONS

1. The problem of modeling the volume laser-induced phase transformations is discussed.
2. The experimental data of creation the cascade changes in laser-irradiated 4H-SiC are analyzed.
3. The modivied Rayleygh model and generalizing Lugovoy-Prokhorov theory of moving foci allows explaining the cascade nature of these experimental data.
4. Modified Rayleygh model are used for the explanation of the microscopic properties of created structures determination of sizes and forms of nanovoids.

5. Possible application the cascade model for the explanation these results is analyzed too.
6. Thus, in this paper, we analyzed the nonlinear optical phenomenon of self-focusing and Cherenkov radiation. The basic models that describe these phenomena are given.
7. Based on the microscopic N. Bohr and A. Bohr model, it was shown that the Cherenkov radiation and the conical radiation of self-focusing are of a similar nature and are due to the inhomogeneous polarizability of the matter.
8. It is also suggested that the phenomenon of the formation of laser-induced breakdown in irradiated dielectrics can be represented as a filamentation phenomenon and methods of Relaxed Optics should be used to describe it.

REFERENCES

[1] Trokhimchuck P.P. (2015) Relaxed Optics: Necessity of Creation and Problems of Development. IJARPS, Vol. 2 , Is. 3, 22-33

[2] Trokhimchuck P.P. (2013) Nonlinear and Relaxed Optical Processes. Problems of Interactions, Vezha-Print, Lutsk.

[3] Trokhimchuck P. P. (2012) Problem of saturation of excitation in Relaxed Optics. JOAM, Vol. 14, **Is**.2-3, 363–370.

[4] Trokhimchuck P. P. (2013) Nonlinear and Relaxed Optical Processes. Problems of Interactions, Vezha-Print, Lutsk

[5] Trokhimchuck P. P. (2018) Problems of modeling the phase transformations in Nonlinear and Relaxed Optics (review). IJERD, Vol.14, Is.2, 48-61.

[6] Haken H. Synergetics. (1977) Springer-Verlag, Berlin-Heidelberg-New York

[7] Hersher M. (1964) Laser-induced damage in transparent media. JOSA, Vol.54, Is.4, 1964, 563-567\

[8] Sharma B. S. (1968) Laser-induced dielectric breakdown and mechanical damage in silicate glasses. Ph. D. Thesis, Simon Fraser University Press, Burnaby

[9] Okada T., Tomita T., Matsuo S., Hashimoto S., Ishida Y., Kiyama S. and Takahashi T. (2009) Formation of periodic strain layers associated with nanovoids inside a silicon carbide single crystal induced by femtosecond laser irradiation. J. Appl. Phys, Vol. 106, Is.5, 054307. 5 p.

[10] Okada T., Tomita T., Matsuo S., Hashimoto, Kashino S. and Ito T. (2012) Formation of nanovoids in femtosecond laser irradiated single crystal silicon carbide. Material Science Forum. –Vol. 725, 19 – 22.

[11] Self-Focusing: Past and Present. (2009) Eds. R.W.Boyd, S.G. Lukishova, Y.-R. Shen, Springer Series: Topics in Applied Physics , Vol. 114., New York, Springer, 605 p.

[12] Lugovoy V. N. and Prokhorov A. M. (1973) Theory of Propagation the Power Laser Irradiation in Nonlinear Matter. Uspekhi Fizicheskikh Nauk, Vol. 111, Is. 2, 203-247. (in Russian)

[13] Chekalin S. V. and Kandidov V. P. (2013) From Self-Focusing Light Beams to Femtosecond Laser Pulse Filamentation. Uspekhi Fizicheskikh Nauk, Vol. 56, Is.2, 133-152. (in Russian)

[14] Shen Y. R. (1975) Self-focusing: experimental. Progr. Quant. Electr., Vol.4, 1975, pp. 1-34.

[15] Murburger H. (1975) Self-focusing: theory. Progr. Quant. Electr., Vol.4, 35-110.

[16] Juhash T. G., Kastis G. A., Suares C., Borand Z. and Bron W. E. (1996) Time-Resolved Observations of Shock Waves and Cavitation Bubbles Generated by Femtosecond Laser Pulses in Corneal Tissue and Water. Lasers in Surgery and Medicine. Vol. 19, 23 – 31.

[17] Lauteborn W. and Kurz T. (2010) Physics of bubble oscillations. Rep. Progr. Phys. Vol. 77, 106501, 88 p.

[18] Rayleygh (1894) Theory of Sound, vol. I, Macmillan and Co., London @ New York

[19] Rayleygh (1894) Theory of Sound, vol. II, Macmillan and Co., London @ New York

[20] Rayleygh (1917) On the pressure developed in a Liquid during the Collapse of a Spherical Cavity, Philosophical Magazine and Journal of Science, Vol. 34, Is. 200, 94-98.

[21] Bohr N. (1950) The passage of charged particles through matter, IL, Moscow (In Russian)

[22] Bohr A. (1950) Influence of Atomic Interaction on the Passage of Atomic Particles through Matter, in: Bohr N. The passage of charged particles through matter, IL, Moscow, 105 -144. (In Russian)

[23] Frank I. M. (1988) Cherenkov Radiation. Theoretical Aspects, Nauka, Moscow (In Russian).

[24] Kobzev A. P. (2010) Cherenkov radiation mechanism. EPAN, Vol.41, Is.3, 830-867 (In Russian)

[25] M. Birnbaum, Semiconductor surface damage produced by Ruby Laser, J. App. Phys., vol. 36, Is.11, 1965, 3688–3689.

[26] Stuart B. S., Feit M. D., Rubenchik A. M., Shore B. W. and Perry M. D. (1995) Laser-Induced Damage in Dielectrics with Nanosecond to Subpicosecond Pulses. Phys. Rev. Lett., Vol. 74, Is.12, 2248-2252.

[27] Boyd R. W. (2008) Nonlinear Optics, Elsevier Publishing, Amsterdam a. o.

[28] Shen Y.R. (2002) Principles of nonlinear optics, Wiley Interscience, Ney-York a. o.

[29] Trokhimchuck P. P. (2007) Radiation Physics of Status Solid, Vezha, Lutsk (In Ukrainian)

[30] Manenkov A. A, Prokhorov A. M. (1986) Laser Destruction of Transparent Solid. Uspekhi Fizicheskikh Nauk, Vol. 145, Is. 1, 179-211 (in Russian)

[31] Trokhimchuck P. P. (2017) Problems of reradiation and reabsorption in Nonlinear and Relaxed Optics/ IJARPS, Vol. 4, Is. 2, 37-50

[32] Philips J.C. (1981) Metastable honeycomb model of laser annealing.//Journal of Applied Physics, No.12, Vol. 52, 7397-7402.

[33] Trokhimchuck P. P. (2014) Self-focusing and Cherenkov Radiation. Electronics-INFO, Is. 1, 32-34 (In Russian)

[34] Ahuja R., Ferreira da Silva A., Persson C., Osorio-Gullién G., Pepe I., Järendahl K., Lindquist O. P. A., Edwards N. V., Wahab Q. and Johansson B. (2002) Optical Properties of 4H-SiC. J. Appl. Phys., Vol. 91, Is. 4, 2099 – 2103.

[35] Ryndya S. M. (2014) Peculiarities of Thin Films SiC structure, which is formatted on Si and Al_2O_3 substrates by method of pulse laser precipitation. Ph. D. Thesis. L. Ya Karpov Scintific Research Physical-Chemical Institute, Moscow (In Russian)\

[36] Moskovskikh D. O. (2015) Production of Submicrometer Powder of Silicon Carbide and Nanostructural Ceramics on its Basis. Ph. D. Thesis. National Research Technological University Steel and Alloys, Moscow (In Russian)

[37] Ki-Taek Byun and Ho-Young Kwak (2004) A model of laser-induced cavitation. Jap. J. Appl. Phys., Vol. 43, Is. 2, 621-630

[38] Potemkin F.V., Mareev E. I. (2013) Shock waves and cavitation bubbles dynamics as a function of the tightly focused femtosecond laser energy in distilled water and acetone. Scientific Notes of Physical Faculty. Mikhail Lomonosov Moscow State University, 133401, 9 p. (In Russian)

[39] Vakhnenko V. O. and Vakhnenko O. O. (2016) Wave Dynamics of Structural Matter,: Naukova Dumka, Kyiv (In Ukrainian)

[40] Trokhimchuck P. P. (2018) Problems of modeling the phase transformations in Relaxed Optics. Proc. X-th Int. Conf. “Fundamental Problems of Optics”, 15-19 October 2018, University ITMO Publishing, Saint-Petersburgh, 173-175 (In Russian)

[41] Trokhimchuck P. P. (2018) Continuum Mechanics, Vezha-Print, Lutsk (In Ukrainian)

Citation: *Petro P. Trokhimchuck , "Some Problems of Modeling the Volume Processes of Relaxed Optics", International Journal of Advanced Research in Physical Science (IJARPS), vol. 5, no. 11, pp. 1-14, 2018.*